Determination of water quality parameters using imaging spectrometry – case study for the Sajó floodplain, Hungary .

Ulanbek Turdukulov[a&b], Zoltán Vekerdy[b]
[a] Kyrgyz State National University, Geographical faculty, Abdymomunov str., 328, 720024, Bishkek, Kyrgyz Republic
[b] Institute for Geo-Information Science and Earth Observation (ITC), P.O. Box 6, 7500AA, Enschede, The Netherlands

ABSTRACT

This study investigates approaches of quantification of water quality parameters (TSM and CHL) using imaging spectrometry. The method is based on field spectrometry measurements, which were up-scaled to the spectral resolution of hyperspectral airborne sensors (ROSIS, DAIS) flown over the Sajó floodplain (Hungary) as part of the HYSENSE 2002 project. Empirical and simplified bio-optical algorithms were applied to each sensor in order to retrieve the concentrations of the water constituents. The results of the analysis indicate that for CHL an empirical algorithm, based on band ratio NIR/Red shows high correlation. To quantify TSM, an inversion of a simplified bio-optical model in the NIR region was applied. The modelling results indicated that the SIOPs of the Sajó River were changing with time due to flood retreat. Proper modelling required the separation of the scattering by large and small-suspended particles. In lack of direct measurements, the suspended particle size was calculated as a function of the river velocity.

ABBREVIATIONS

CDOM	Concentration of Dissolved Organic Matter
CHL	Chlorophyll-a
ISM	Inorganic Suspended Matter
OSM	Organic Suspended Matter
SIOP	Specific Inherent Optical Properties
TSM	Total Suspended Matter
WQ	Water Quality

1. INTRODUCTION

TSM and CHL are important WQ parameters related to the total primary production and fluxes of heavy metals and micro pollutants. Conventional measurements of these parameters require *in situ* sampling and expensive and time-consuming laboratory work. Due to these limitations, the sampling size often cannot be large enough to cover the entire water body. Therefore the difficulty of synoptic and successive water quality sampling becomes a barrier to water quality monitoring and forecasting [1].

In the present research we aim to test statistical and simple bio-optical modelling algorithms for WQ retrieval based on field spectrometry collected from Dutch water bodies, validate those algorithms on the field spectrometry measurements made on the Sajó floodplain and eventually apply the algorithms to the airborne hyperspectral data (ROSIS and DASI sensors) acquired as a part of the HYSENSE 2002 project.

The Sajó River basin is one of the most industrialized regions in Hungary. Consequently, pollution has been a serious problem for many years. Although in the recent years some of the factories were closed down, short-term peak contamination as well as shifts to new chemicals can be observed continuously [2]. Thus, the region is still in need of a good monitoring system for water quality, as the river is the main medium of pollution transport. It is particularly important in relevance to the Hungarian accession to the European Union.

Presented at the 3rd EARSeL Workshop on Imaging Spectroscopy, Herrsching, 13-16 May 2003

2. FIELD SPECTROMETRY MEASUREMENTS

The dataset consists of subsurface spectra taken from the Dutch inland water bodies by the Institute of Environmental Studies (IVM) of Free University Amsterdam (VU) with a kind permission to use them in this research. Subsurface spectra were collected with spectrometer PR650-1 having range from 380 to 780 nm with 4 nm intervals. The number of measurements taken in cloudless condition was 34. Along with the spectra, the following WQ parameters were measured: TSM, ISM, OSM, CHL, Secchi depth, CDOM (**Table 1**). Detailed information on the process of the Dutch subsurface spectra collection could be found, for example in [3].

In Hungary, field spectrometry measurements were carried out from 20 to 25 August 2002 along a reach of the Sajó River, Hungary. All the measurements were performed on a flat-water surface and in sunny condition. The following measurements were made:

- Upwelling radiance spectra of the water bodies with the sensor (spectrometer GER 3700, fibre optics with 23^0 FOV, with about 1.5 nm interval) viewing the water surface vertically (30 cm above the water surface). Nine measurements were taken from each site consecutively, which were later averaged to minimize random effects
- Downwelling radiance spectrum was measured with a reference panel (Barium sulphate plate with approximately 100% reflectance, 20 cm above the panel);
- Reflectance spectra of the water body was calculated (ratio of the upwelling radiance of the water and that of a reference panel);
- Water samples were taken at 0.2 m depth in order to analyse them for water quality parameters (TSM, ISM, OSM, CHL, Secchi depth).

The in *situ* measurements have been taken in 15 points. Analysis results show large variances and standard deviations of the parameters because of a few high values. This was due to the difficulty of finding water bodies with gradual changes in the water quality parameters. The same reason limited the number of measurements to 15.

	CHL range (μg/l)	*TSM range (mg/l)*	*Secchi Disc depth, m*	*Depth, m*
NL	0.63- 166.62	1.22- 53.10	0.2-5.0	0.7-40.0
HU	0.89- 138.45	5- 120	0.51-2.36	0.9-8.1

Table 1. Range of WQ parameters measured in both datasets.

In order not to confuse the reader, from now on spectra from Dutch lakes will be named as "Dutch dataset" and field spectra collected In Sajó river floodplain will be called "Hungarian dataset". Both datasets were resampled to the resolution of spectrometer PR650-1, ROSIS and DAIS sensors using central wavelengths and Full-Half-Width-Maximum (FHWM) of above-mentioned sensors.

3. METHODS

Generally, there are two different approaches to estimate the concentrations of WQ parameters from the remote sensing reflectance namely, empirical (also called statistical), and (semi) analytical approach (also called bio-optical modelling, [4]).

3.1. Statistical approach

In the Dutch dataset, chlorophyll-a shows two diagnostic absorption bands centred at around 440 and 675 nm (**Figure 1**). The reflectance peaks at around 550 and 705 nm rise with increasing chlorophyll concentration. Knowing that reflectance peak at 550 nm is affected by the absorption properties of TSM and CDOM, in present research we utilise the statistical approach for CHL determination by using well-established band ratio NIR/Red algorithm.

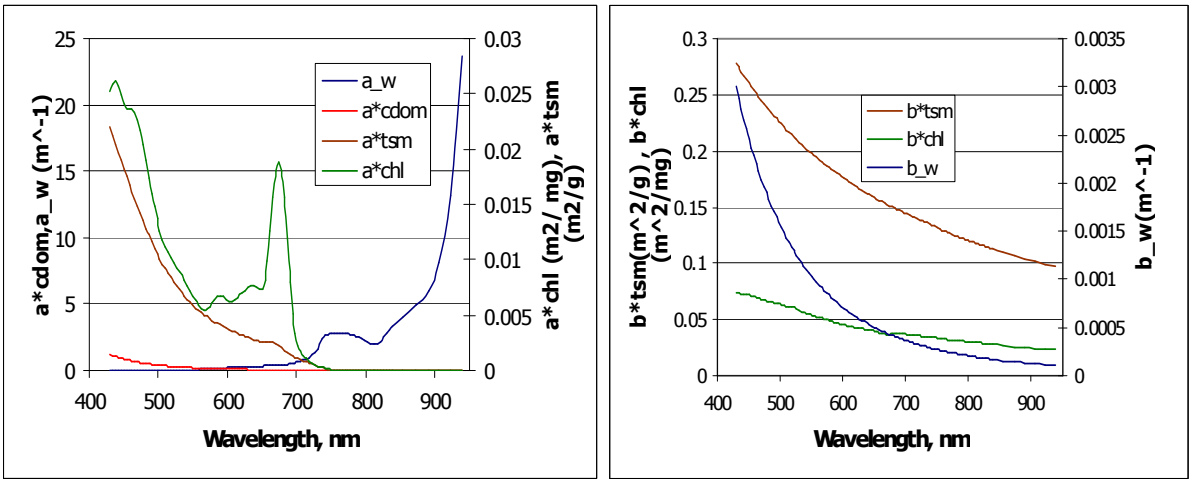

Figure 1. Mean specific absorption (left) and scattering (right) coefficients of the Dutch lakes (Adopted from BIOPTI 1.0, Erin Hogenboom, 1995)

Principally, an occurrence of only TSM in the water increases reflectance along the whole spectrum, but the presence of other constituents, such as CDOM, CHL and the water itself with their absorption and scattering properties (**Figure 1**), makes the statistical quantification of TSM a difficult task. The main information about TSM is scattering, since its absorption has the same shape as CDOM (though much lower in the magnitude). There is a small window (around 700 nm) between the absorption of CHL and the absorption of water (**Figure 1**) where the scattering of TSM can be "visible" using statistical approach.

Bio-optical modelling requires knowledge of specific inherent optical properties (SIOPs) of studied water bodies. However, in this study we did not measure SIOPs of the Hungarian datasets, instead we have used SIOPs from the Dutch lakes (**Figure 1**). Also, for bio-optical modellig we need to transfer remote sensing reflectance above water surface to subsurface reflectance (below the water surface). Given transformation is usually done by corrections for the air-water interface. In this study, we applied air-water interface correction formula of Morel &Gentili [5] to the Hungarian dataset.

3.2. Air-water interface correction algorithm

Morel &Gentili [5] used equation (1) to express the relation between remote sensing reflectance and subsurface reflectance, which we solved for subsurface reflectance:

$$R_{rs} = \frac{(1-\rho)*(1-\rho')*R(0-)}{1-r*R(0-)*n^2*Q} + R_{surf} \quad (1)$$

Where, R_{rs} is the remote sensing reflectance (sr^{-1});
$R(0-)$ is the subsurface reflectance (unitless);
R_{surf} is a specular reflectance from the surface of the water body (sr^{-1});
Q is a ratio of upwelling irradiance to upwelling radiance (5 sr);
ρ is an internal Fresnel reflectance (0.03);
ρ ' is an air-water Fresnel reflection at the interface (0.54);
n- refractive index of water (1.34) ;
r-water-air reflection (0.54).

Default values indicated in the brackets of the key of equation (1) are taken from the WASI 2.0 (Water Colour Simulator) software [6].

Upwelling spectra measured above the water can be affected by sun glint from the water surface (specular reflectance, R_{surf}) due to waves or foam (**Figure 2**). In order to detect R_{surf} in measured spectra, we followed the assumption that the light absorption by pure water is predominant in NIR (970-1000 nm) and the water-leaving radiance in that region is zero [7].

Considering the gradually increasing noise in the collected spectra, we found minimum reflectance in Hungarian dataset at 950 nm. The reflectance value at this wavelength was used to remove specular reflectance and wave effects (assuming that they are wavelength independent) by subtracting it from the whole spectra.

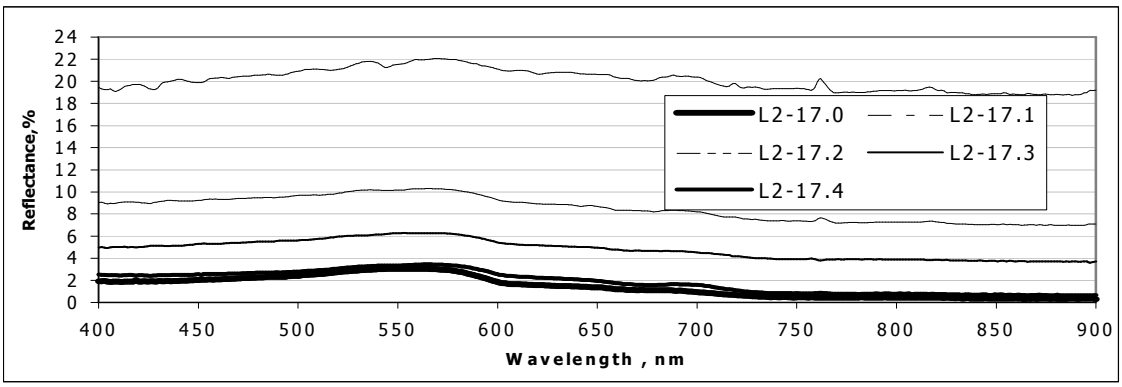

Figure 2. Effect of waves on the successive spectral measurements at the sampling point L2 on 17th August

3.3. Simplified bio-optical model

We applied the Gordon model [8] with following assumptions [9], [10]:

- Absorption in the NIR is only due to the absorption of water
- Backscattering in the NIR is due to the backscattering of water, TSM and CHL

$$R(0-) = f\,\frac{b_b}{a + b_b} \tag{2}$$

$$b_b = b_w * B_w + b^*_{tsm} * B_{tsm} * TSM + b^*_{chl} * B_{chl} * CHL \quad \text{and} \quad a = a_w;$$

where, $R(0-)$ is the volume reflectance at N^{th} band in NIR region (unit less);
f is the proportionality factor related to the illumination condition and viewing geometry (unit less, f=0.33, [9], [11]);
b_b is the total backscattering coefficient (m^{-1});
a is the total absorption coefficient (m^{-1});
a_w , b_w are absorption and scattering coefficients of pure water (m^{-1});
TSM and CHL are the concentrations of TSM and CHL (mg/l and µg/l);
B_w, B_{tsm}, B_{chl} are the probabilities that light will backscatter back to the sensor from a given water constituent (unit less);
b^*_{tsm} and b^*_{chl} is the specific scattering coefficients of TSM and CHL respectively (m^2/g and m^2/mg respectively);

Substituting as:

$b_{b\_tsm} = b^*_{tsm} * B_{tsm} * TSM$, where b_{b_tsm} is a total backscattering by TSM only,
$b_{b\_chl} = b^*_{chl} * B_{chl} * CHL$, where b_{b_chl} is a total backscattering by CHL only,

and solving (2) for TSM in the NIR region leads to the following expression:

$$b_{b\_tsm} = \frac{f * b_w * B_w + f * b_{b\_chl} - R(0-) * b_{b\_chl} - R(0-) * (a_w + b_w * B_w)}{R(0-) - f} \tag{3}$$

$$TSM = \frac{b_{b\_tsm}}{b^*_{tsm} * B_{tsm}}$$

For CHL determination using bio-optical model we used formula proposed by Gons [12]. Essentially it is bio-optically modeled band ratio 704/672 nm:

$$CHL = \frac{BR * (a_w^{(704)} + b_b) - a_w^{(672)} - b_b}{a_{chl}^{*(672)}} \tag{4}$$

Where b_b values we assumed to be equal to b_{b_tsm} as described in the equation (3) and *BR* is the band ratio.

4. RESULTS

4.1. Results of the statistical analysis: CHL

Results indicate the highest regression coefficients for CHL retrieval at different spectral locations: in Dutch dataset NIR/Red wavelengths are 712/664 nm whereas in Hungarian datasets the wavelengths are 704/676 nm (**Table 2**). However high agreement was found in slope and intercept values of the regression lines of the two datasets when using the ratio of 704/672 nm of remote sensing reflectance of Hungarian dataset (**Table 2**, **Figure 3** –applied to the ROSIS sensor). Since the CHL range was not covered homogeneously, an outlier in the Hungarian dataset affects the regression coefficient: by removing it from **Figure 3** for example, regression coefficient reduces to 0.87 but it still shows strong correlation

	Sensor: PR650-1	*Wavelengths, nm*	r^2	*Slope*	*Intercept*
1	NL: *R(0-)*	712/664	0.94	94.08	-50.99
2	NL: *R(0-)*	704/672	0.91	71.03	-48.00
3	HU: *R(0-)*	704/676	0.98	57.03	-44.28
4	HU: *R(0-)*	704/672	0.97	63.56	-50.85
5	HU: R_{rs}	704/672	0.98	66.98	-54.85

Table 2. Result of applying statistical band ratio algorithms for CHL retrieval for both datasets

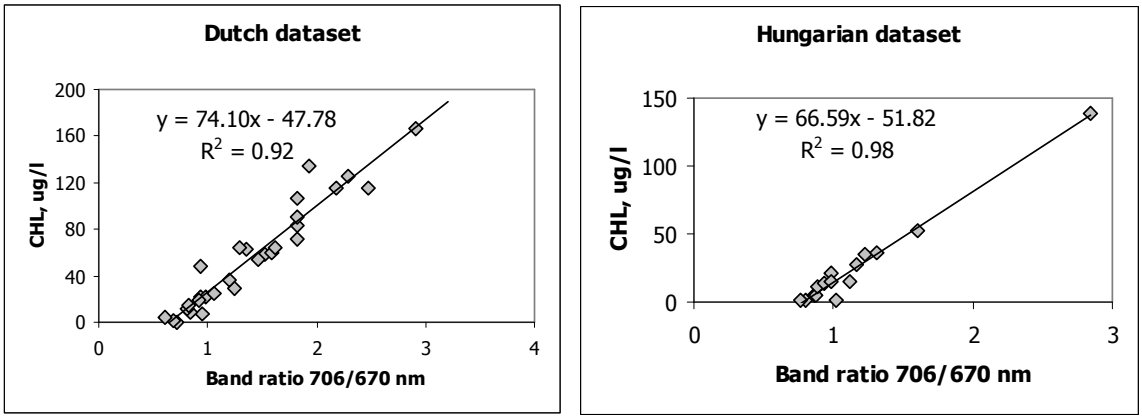

Figure 3. Band ratio 706/670 nm versus CHL applied to the characteristics of the ROSIS sensor

Statistical analysis of TSM yielded two different algorithms for TSM retrieval in the two datasets at different spectral locations (**Table 3**), showing different source of TSM present in the sampling sites.

Sensor: PR650-1	*Regression function*	*Wavelength, nm*	r^2	*Slope*	*Intercept*
NL: *R(0-), %*	Linear	724	0.84	0.14	0.47
HU: *R(0-), %*	LN (TSM)	664	0.84	0.40	1.06
HU: R_{rs}, *%*	LN (TSM)	688	0.88	0.49	1.05

Table 3.Summary of the statistical analysis of TSM and single band reflectance for two datasets

Thus, it is rather difficult to predict the exact wavelength where the highest correlation can occur using statistical approach for TSM determination. The algorithm is also affected by the number of measurements and by the origin of TSM present in the studied waters: TSM consisting mainly of phytoplankton cells will have more absorption at 680 nm and subsequently there would be a shift of algorithm towards longer wavelengths, as in the case of the Dutch dataset.

Nevertheless, the overall results indicate that the Gons formula could be used for the monitoring of CHL since it is an essentially simplified "physical" model. Gons [12] proposed to use of his algorithm for the waters with a wider range of CHL concentrations (from 1 to 215 mg/l) than we observed in the study area. In addition, the appliance of the band ratio makes the model to be relatively insensitive to the proportionality factor, *f,* and consequently to the illumination conditions. All above makes the algorithm independent from in situ calibration data, which is always needed for the statistical approach.

4.2. Results of the simplified bio-optical modelling: CHL

Bio-optical modelling of the band ratio gives results close to the observed ones, though algorithm underestimated CHL concentrations for the Dutch dataset (**Table 4**.).

	Sensor: PR650-1	*Wavelengths, nm*	r^2	*Slope*	*Intercept*
1	NL: *R(0-)*	704/672	0.91	1.48	7.06
2	HU: *R(0-)*	704/672	0.97	1.02	2.09

Table 4. Bio-optically modelled vs. observed CHL for both datasets (sensor PR650-1).

Nevertheless, the overall results indicate that the Gons formula could be used for the monitoring of CHL since it is an essentially simplified "physical" model. Gons [12] proposed to use of his algorithm for the waters with higher CHL concentrations than we observed in the study area (from 1 to 215 mg/l). In addition, the appliance of the band ratio makes the model to be relatively insensitive to the proportionality factor, *f,* and consequently to the illumination conditions. All above makes the algorithm independent from in situ calibration data, which is always needed for the statistical approach.

4.3. Results of the simplified bio-optical modelling: TSM

In Dutch dataset modelling gave generally good results (**Figure 4**). In Hungarian dataset initially modelling was performed using the mean specific scattering coefficients of the Dutch inland waters. Results indicated poor correlation between modelled and observed TSM concentrations for the whole Hungarian data set. However, an analysis of the obtained results showed that overall regression coefficients were low due to the modelled TSM from the rivers only.

Further, by trying to find out the "best fit" specific scattering coefficients for River Sajó revealed that the scattering of TSM is changing with time (it required 3 different sets of scattering coefficients for the rivers on 20th, 24th and 25th August). During the airborne imaging flight on 17th August, the Sajó River had a higher flow velocity than on the other sampling dates, because the river stage was dropping after a flood peak. Since the particle size of the suspended matter is proportional to the flow velocity, which is decreasing with the descent of the river stage after flood. This leads to the conclusion that the river's TSM backscattering is influenced by the particle size of the suspended matter.

Gege [6] used two different sets of backscattering coefficients for modelling TSM in Lake Constance: backscattering by large and small particles where the first one is wavelength independent. To define the terms large and small Van de Hulst [13] suggested that backscattering is wavelength independent if particles are "much larger" than the wavelength. Assuming roughly that "much larger" means a factor of 10, than particles sizes should be above 0.01 mm for the spectral region around 1000 nm (NIR). Thus, introducing specific backscattering by large and small particles leads equation (3) to the following (Gege, 2001):

$$TSM_{large} = \frac{b_{b\_tsm}}{b^*_{b\_tsm\_large} + \frac{b^*_{b\_tsm\_small}}{r}} \qquad (5)$$

$$TSM_{small} = \frac{TSM_{large}}{r}$$

where,

$b^*_{b\_tsm\_large}$ is a specific backscattering by large particles of TSM (m^2/g);
$b^*_{b\_tsm\_small}$ is a specific backscattering by small TSM particles (m^2/g);
r is a ratio of large particle's concentration to small particle's concentration (unit less);
TSM_{large} *and* TSM_{small} are the concentrations of large and small TSM particles respectively (mg/l).

A study undertaken jointly by RIZA and VITUKI [2] illustrated that at the average diameter of suspended sediment in Sajó River is 0.04 mm. About 30% of the suspended sediment is falling into the fine sand category (between 0.05 and 0.1 mm) and about 10% is finer than 0.006 mm. Assuming the exponential function of flood retrieving from 17th August (high flow) to 25th August (low flow) with an average of 27% of small particles (finer than 0.01 mm), following *r* values were used for further modelling:

Date	Ratio of large to small particle's concentration, ***r***	Percentage of large particle's concentration	Percentage of small particle's concentration
17	4.79	83	17
18	4.19	81	19
19	3.66	79	21
20	3.20	76	24
21	2.796	74	26
22	2.44	71	29
23	2.13	68	32
24	1.86	65	35
25	1.63	62	38
Average		73%	27%

Table 5. Assumption values of ratio of large to small particle's concentration in the Sajó River during the flood retreat

Table 6 shows input parameters (besides the remote sensing reflectance corrected for air-water interface) used for the TSM modelling using DAIS sensor's properties:

Wavelength, nm	a_w	b_w	$b^*_{tsm\_small}$	$b^*_{tsm\_large}$	b^*_{chl}	Constants:	
747	2.498243	0.000277	0.13247	0.01	0.033556	B_{tsm}	0.06 [9]
766	2.709976	0.000248	0.127604	0.01	0.03207	B_w	0.5 [9]
783	2.564723	0.000226	0.123799	0.01	0.031035	B_{chl}	0.016 [9]
802	2.22497	0.000203	0.11987	0.01	0.029988	f	0.33 [11]

Table 6. Input parameters for TSM modelling (resampled to the DAIS sensor)

Thus, by using the above estimated ratio of concentration of large to small particles, mean specific scattering by small particles from the Dutch lakes, specific scattering by large particles from Lake Constance and mean specific scattering of CHL from the Dutch lakes, the following results were obtained from modelling of TSM (**Figure 4**):

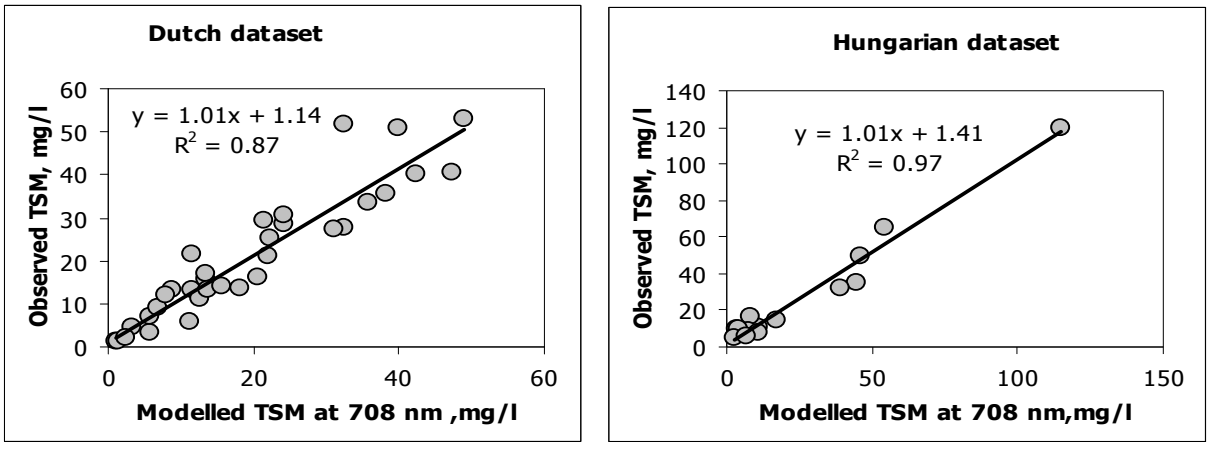

Figure 4. Regression graphs between observed and modelled at 708 nm TSM concentrations (sensor: PR650-1)

5. APPLICATION OF THE RESULTS TO THE HYPERSPECTRAL IMAGES

Flights took place on 17th and 18th August over the Sajó floodplain. Weather conditions on 18th August were more appropriate for the water quality monitoring (absence of clouds and wind). Regrettably, due to an internal error in the performance of the ROSIS sensor, only the atmospheric correction (apart from the geometric correction) of the ROSIS image from 17th August could be performed. For the same reason, the ROSIS sensor failed to acquire an image on 18th August. Regarding the DAIS sensor, it performed well in both days and for the analysis we used the atmospherically and geometrically corrected DAIS image from 18th August.

Atmospheric correction of the images was tuned by applying empirical line calibration method to match them with field spectra measurements. Further, the system noise on the images was eliminated (preserving spatial variation) by applying a smoothing (low pass convolution) filter with a kernel size of [5*5].

For CHL determination we applied two algorithms: statistical band ratio to the ROSIS image and bio-optically modelled band ratio to the DAIS image. For TSM determination we used simplified bio-optical modelling described in the previous section.

Essentially, two CHL maps (**Figure 5**) gave the same order of magnitude and pattern of the CHL distribution. Only a little variation exists between the river and the lakes: this is the result of the previous flood, which washed through the lakes on the floodplain either directly, or via the groundwater. TSM map (**Figure 5**) shows that the river Sajó and its tributary, the Hernád had higher values of TSM than the surrounding lakes. As the DAIS image was from 18th August, the TSM concentrations in the river are generally higher than those that were observed on 20th and later. It consents with the higher flow velocity and the capacity to carry more sediment during the high flow on 18th August. Also the map agrees with the fact that there was a direct surface inflow from the river into lakes on south side during the flood. The TSM distribution shows higher values at the shores of rivers and lakes possibly due to the bottom reflectance or/and due to the applied smoothing filter.

6. CONCLUSIONS

The empirical approach, particularly the proposed band ratio algorithms for the modelling CHL was found to be sufficiently accurate. The developed statistical relationships have been tested on both data sets (total N=44). The ANOVA test performed on both trend lines of **Figure 4** showed absence of a significant variation between two trend lines (N=44,α =0.05, p=0.37). Additionally, the developed models are similar to the ones found by other researches, for example, in Thiemann and Kaufmann, [14]: *CHL = 73.59*BR (R705nm/R678nm)-52.9*1.

Results of bio-optical modelling indicate that the Gons formula could be used for the monitoring of CHL since it is an essentially simplified "physical" model. Analysis of results for different sensors reviled that both band ratio algorithms (the statistical approach and the bio-optical modelling) are very sensitive to the precise detection of the CHL absorption peak at 675 nm and the following reflectance peak at 705 nm.

In bio-optical modelling of TSM, in the Equation (3) it is possible to assume that in NIR region backscattering is chlorophyll independent (b_{b_chl} = 0). The results obtained using this modification are almost identical to the previously described ones, with slightly higher slope and intercept values and slightly lower regression coefficients (r^2=0.84 for the Dutch dataset). This leads to the conclusion that introduction of b_{b_chl} improves model for CHL dominant type of water bodies, as they are in Dutch dataset.

Generally, the use of other SIOPs than the ones determined from the studied water bodies can be a source of errors. However, in the absence of direct data from the Hungarian sites, we used SIOPs from the Dutch lakes. The results of bio-optical modelling of TSM indicate similarity between the SIOPs of the inland waters (mostly lakes) in Holland and the lakes in the study area.

The water of the Sajó River, due to its high TSM values with a wide range of grain sizes, required a different approach – the separation between the large and small-suspended particles.

Although it is intuitively right to assume that the river's TSM backscattering depends on the particle size (which is a function of the flow velocity), essentially our assumption was based on only 5 measurements in the rivers. It can be concluded that direct measurements of SIOPs in the study area will increase the accuracy of the bio-optical-modelling for both TSM and CHL. Furthermore, a study of the relation between the flow velocity and particle size and subsequently the backscattering properties of the particles will greatly contribute to the understanding of the river's reflectance properties and later to the better bio-optical modelling of TSM and CHL in the rivers.

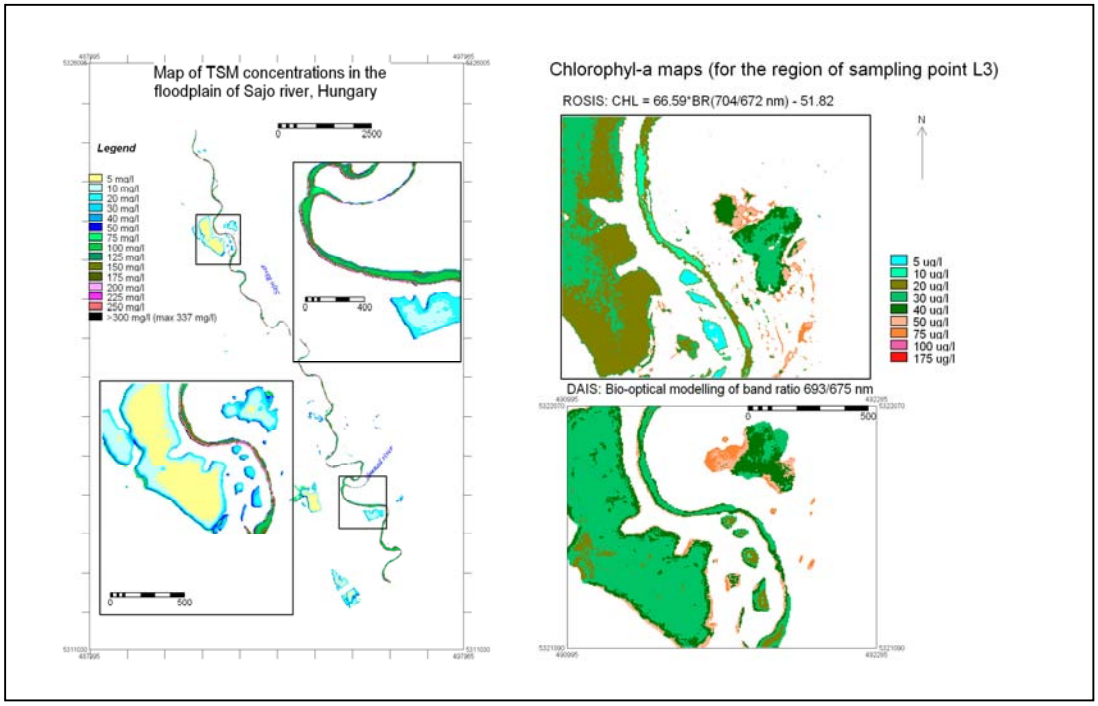

Figure 5. Resulting TSM and CHL maps. Note that the ROSIS image is not corrected geometrically.

ACNOWELEDGMENTS

Authors are highly grateful to the Institute of Environmental Studies (IVM) of Free University Amsterdam (VU), especially to Dr. Steef Peters, for the kind permission to use the subsurface reflectance spectra of Dutch inland waters and for providing thorough guidance throughout the research; to WRS department of International Institute for Geo-Information Science and Earth Observation (ITC) particularly to Dr. Chris Mannaerts, for financing the presentation of the article at the 3rd EARSEL workshop.

REFERENCES

[1] SHAFIQUE, N. A., B. C. AUTREY, FULK, F., CORMIER, S. M., 2001: The Selection of Narrow Wavebands for Optimizing Water Quality Monitoring on the Great Miami River, Ohio using Hyperspectral Remote Sensor Data. *Journal of Spatial Hydrology 1(1)*, pp.1-22.

[2] RIZA, VITUKI, 1994: Ecological Rehabilitation of Floodplains of Rivers, Report of the Institute for Water Pollution Control, the Netherlands (RIZA) and the Water Research Center (VITUKI), Hungary.

[3] DE HAAN, J. F., KOKKE J. M. M., DEKKER, A. G., RIJKEBOER, M., 1999: Remote Sensing Algorithm Development: toolkit for water quality continued. Delft, Report of the Netherlands Remote Sensing Board (BCRS), pp. 88.

[4] KRIJGSMAN, J., 1994: Optical properties of Water Quality parameters. Interpretation of Reflectance Spectra, PhD thesis, Delft University of Technology, pp. 200.

[5] MOREL, A., GENTILI, B., 1993: Diffuse reflectance of oceanic waters: II. Bidirectional aspects. *Applied Optics 32*: pp. 6864-6879.

[6] GEGE, P., 2002: WASI 2.0 User manual, Oberfaffenhofen, pp. 59

[7] OUILLON, S., FORGET, P., FROIDEFOND, J.M., NAUDIN, J.J., 1997: Estimating suspended matter concentrations from SPOT data and from field measurements in the Rhone river plume. *Marine Technology Society Journal 31(2)*, pp. 15-20.

[8] GORDON, H. R., BROWN, O. B., JACOBS, M.M., 1975: Computed relationship between the inherent and apparent optical properties of a flat homogeneous ocean. *Applied Optics 14(2)*, pp. 417-427.

[9] BUKATA, R. P., JEROME, J. H., KONDRATYEV, K.Y., POZDNYAKOV, D.V., 1995: Optical properties and Remote Sensing of Inland and Coastal Waters, CRC Press, New York.

[10] Babin, M., Stramski D., 2002: Light absorption by aquatic particles in the near-infrared spectral region. *Limnology and Oceanography 47(3)*, pp. 911-915.

[11] DEKKER, A. G., 1993: Detection of optical water quality parameters for euthrophic waters by high-resolution remote sensing, PhD thesis, Free University Amsterdam, pp. 240.
[12] GONS, H. J., 1999: Optical teledetection of Chlorophyll-a in Turbid Inlands Waters. *Environmental Science and Technology 33*, pp. 1127-1132.
[13] VAN DE HULST, H. C., 1957: Light scattering by small particles. Dover, New York.
[14] THIEMANN, S., KAUFMANN, H., 2002: Lake water monitoring using hyperspectral airborne data - a semi-empirical multisensor and multitemporal approach for the Mecklenburg Lake District, Germany. *Remote Sensing of Environment 81,* pp. 228-237.